Hierarchical guidewire tracking in fluoroscopic sequences

Article *in* Proceedings of SPIE - The International Society for Optical Engineering · February 2009

Impact Factor: 0.2 · DOI: 10.1117/12.812508

7 authors, including:

Ying Zhu
Siemens
38 PUBLICATIONS **738** CITATIONS
SEE PROFILE

Wei Zhang
Fudan University
1,001 PUBLICATIONS **13,407** CITATIONS
SEE PROFILE

Hierarchical Guidewire Tracking in Fluoroscopic Sequences

Peng Wang[a], Ying Zhu[a], Wei Zhang[a], Terrence Chen[a], Peter Durlak[b], Ulrich Bill[b] and Dorin Comaniciu [a]

[a]Integrated Data Systems Department, Siemens Corporate Research, 755 College Road East, Princeton NJ, U.S.A.
[b]Siemens MED-AX, Siemensstr. 1, Forchheim, Germany

ABSTRACT

In this paper, we present a novel hierarchical framework of guidewire tracking for image-guided interventions. Our method can automatically and robustly track a guidewire in fluoroscopy sequences during interventional procedures. The method consists of three main components: learning based guidewire segment detection, robust and fast rigid tracking, and non-rigid guidewire tracking. Each component aims to handle guidewire motion at a specific level. The learning based segment detection identifies small segments of a guidewire at the level of individual frames, and provides unique primitive features for subsequent tracking. Based on identified guidewire segments, the rigid tracking method robustly tracks the guidewire across successive frames, assuming that a major motion of guidewire is rigid, mainly caused by the breathing motion and table movement. Finally, a non-rigid tracking algorithm is applied to finely deform the guidewire to provide accurate shape. The presented guidewire tracking method has been evaluated on a test set of 47 sequences with more than 1000 frames. Quantitative evaluation demonstrates that the mean tracking error on the guidewire body is less than 2 pixels. Therefore the presented guidewire tracking method has a great potential for applications in image guided interventions.

Keywords: guidewire tracking, image-guided interventions, fluoroscopy, deformation, performance evaluation

1. INTRODUCTION

In image guided interventions, automatic guidewire tracking has important applications. Since a low dose of radiation and contrast materials is desired, fluoroscopic images captured during interventions usually have low image quality. This leads to the low visibility of vessels, catheters, and guidewires. Automatic guidewire tracking can help to improve the visibility of guidewire, and assist clinicians to obtain the high precision of image-guided interventions. This paper presents a framework, based on our developed machine learning and computer vision algorithms, to automatically and robustly track guidewire in fluoroscopic sequences for image guided interventions.

Guidewire tracking in fluoroscopic sequences is challenging. Guidewires are thin and with low visibility in fluoroscopic images, which usually have poor image quality due to a low dose of radiations in interventional imaging. Some exemplar guidewires are displayed in Fig. 1. Sometimes some segments of guidewires are barely visible in noisy images. Such weak and thin wire structures in noisy images make the robust tracking difficult. Guidewires also exhibit large variations in their appearances, shapes and motions. The shape deformation of a guidewire is mainly due to a patient's breathing and cardiac motions in 3D, but such 3D motions are complicated when being projected onto a 2D image space. Furthermore, there exist many other wire-like structures, such as guiding catheters and ribs. Some of the structures are close to the guidewire, and could distract guidewire tracking and finally lead to tracking failures. All the aforementioned factors, along with robustness and speed requirements for interventions, make guidewire tracking challenging.

Since a guidewire is thin, the tracking methods that use regional features such as holistic intensity, textures, and color histogram,[1] cannot track it well. Active contour[2] and level set[3] based methods, heavily rely on intensity edges, and are

Further author information: (Send correspondence to Peng Wang)
Peng Wang, E-mail: peng-wang@siemens.com
Ying Zhu, Email: yingzhu@siemens.com
Wei Zhang, Email: wei-zhang@siemens.com
Terrence Chen, Email: terrence.chen@simens.com
Peter Durlak, Email: peter.durlak@siemens.com
Ulrich Bill, Email: ulrich.bill@siemens.com
Dorin Comaniciu, Email: dorin.comaniciu@siemens.com

Medical Imaging 2009: Image Processing, edited by Josien P. W. Pluim, Benoit M. Dawant,
Proc. of SPIE Vol. 7259, 72591L · © 2009 SPIE
CCC code: 1605-7422/09/$18 · doi: 10.1117/12.812508

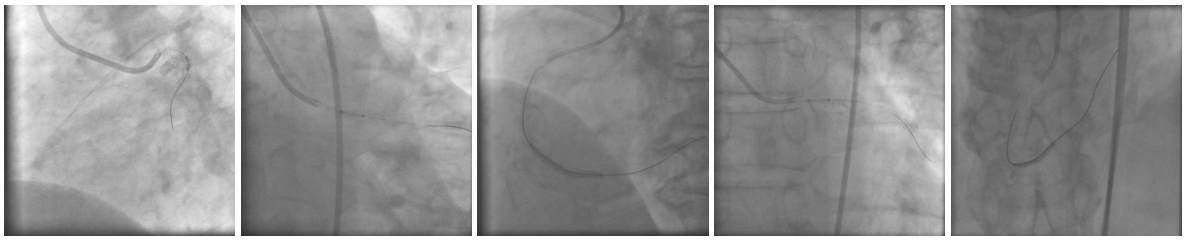

Figure 1. Some exemplar guidewires in fluoroscopic images

easily attracted to image noise and other wire-like structures in fluoroscopy. Considering the noise level in fluoroscopic images, such methods cannot deliver desired speed, accuracy and robustness for interventions. There is some work on the guidewire tracking[4,5] and detection.[6] Beyar et. al.[4] use filter based methods to identify a guidewire in X-ray images, and then use Hough transform to fit a polynomial curve to track a guidewire. There are no quantitative reports on tracking performance in their paper. The method of Baert et. al.[5] tracks guidewire in images enhanced by image subtraction and coherence diffusion. However, their experiments show that only a part of guidewire, not the whole guidewire, have been tracked. Barbu et. al.[6] present a learning based method to automatically detect the whole guidewire in fluoroscopic sequences. The method achieves good performance on individual frames, but has not utilized temporal coherence to continuously identify the guidewire in sequences.

This paper presents a hierarchical framework to continuously and robustly track the guidewire for image guided interventions. The presented framework consists of three main components: learning based guidewire segment detection, rigid tracking, and non-rigid deformation. Each component aims to handle deformations of a guidewire at a specific level. The learning based segment detection automatically identifies small segments of a guidewire at the level of individual frames, and provides unique primitive features for subsequent tracking. Based on identified guidewire segments, the rigid tracking method robustly tracks the guidewire across successive frames, assuming that a major part of the guidewire motion can be approximated as a rigid motion, mainly caused by breathing motions. Finally, a non-rigid tracking algorithm finely deforms the guidewire to provide accurate tracking results. The method has been evaluated on a test set containing 47 sequences with more than 1000 frames. Quantitative evaluation results show that the mean tracking error on the guidewire body is less than 0.4mm. The presented guidewire tracking method has a great potential for cardiac interventions. In the rest of the paper, we introduce the guidewire tracking method in Section 2, and present the quantitative evaluation results in Section 3. Section 4 concludes the paper.

2. HIERARCHICAL GUIDEWIRE TRACKING

In this section, we introduce a hierarchical method of tracking large and non-rigid guidewire motions in fluoroscopic sequences. The tracking framework consists of three main components: learning based guidewire segment detection, rigid tracking, and non-rigid deformation. Each component tackles problems at a specific level, and their combination provides robust tracking results. At each frame of fluoroscopic sequences, a learning based guidewire segment detection method automatically detects small segments of a guidewire. The detected guidewire segments are primitive features for tracking. After guidewire segments have been detected, a hierarchical tracking scheme is applied to robustly track a guidewire. Since the guidewire exhibits large variations in the shape and motion, especially due to projections from 3D to 2D, we hold no assumptions in this method that the 3D projection information is available, and we do not impose any guidewire motion model that depends on 3D information. Instead, this method tries to handle guidewire motions that could be captured from arbitrary directions. For this purpose, our method decomposes the guidewire motion into two major steps: rigid and non-rigid motions, as the guidewire motion caused by the breathing motion can be approximated as a rigid motion in 2D, and the cardiac motion is non-rigid. The decomposed motions are effectively and efficiently recovered in a hierarchical manner.

2.1 Guidewire segment detection

It is critical to properly represent a guidewire for robust tracking. Usually the shape of guidewire can be represented as a spline curve, however, the appearance of guidewire is difficult to distinguish in fluoroscopy due to background noises

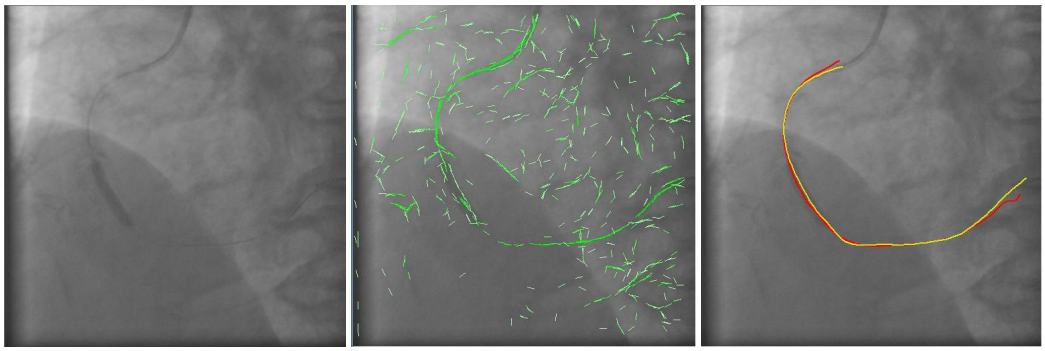

(a) (b) (c)

Figure 2. Hierarchical guidewire tracking. (a): a frame in a fluoroscopic sequence; (b): detected line segments shown in green; (c):tracking results: the guidewire by global and local rigid tracking is shown in red; the yellow line shows the final result after the non-rigid tracking. The figures are best viewed in color

and weak visibility of guidewires. Traditional edge and ridge detectors detect line segments based on derivatives of image intensity, but some thin guidewires may be missed, and many false segments on background will be detected. In this paper, we apply a learning based method that can identify weak guidewire segments, and modestly suppress false detections at background.

A learning method, named probabilistic boosting tree (PBT),[7] is used to build the guidewire segment detector. PBT is a supervised learning method extended from the AdaBoost.[8] The AdaBoost combines multiple weak classifiers into a strong one to achieve satisfying accuracy and speed as well. The PBT further extends original AdaBoost into a tree structure, and is able to model complex distribution of objects, which is desirable in handling different types of guidewires in fluoroscopy. In our method, Haar features[9] are extracted from images as the features used in the PBT classifier. Haar features measure image differences of many configurations, and are fast to compute. For more details about the AdaBoost, PBT and Haar features, please refer to literature.[7–9] For training the guidewire segment detector, we collect thousand of guidewires from fluoroscopic images, and crop segments from the guidewires as the positive training samples, and many image patches outside the guidewires as the negative training samples. The training samples are then used to train the PBT based guidewire segment detector offline.

During detection, the trained guidewire segment detector can identify online if a patch on a given image belongs to a guidewire or the background. The output of a PBT classifier, denoted as $P(\mathbf{x})$ given a image patch at the position $\mathbf{x}$, is a combination of outputs from a collection of learned weak classifiers $H_k(\mathbf{x})$ with associated weights α_k. The numeric outputs can be further interpreted into a probabilistic measurements of guidewire segments,[10] seeing Eqn. (1):

$$\begin{aligned} f(\mathbf{x}) &= \sum_k \alpha_k H_k(\mathbf{x}) \\ P(\mathbf{x}) &\propto \frac{e^{f(\mathbf{x})}}{e^{-f(\mathbf{x})} + e^{f(\mathbf{x})}} \end{aligned} \tag{1}$$

An image patch as the position $\mathbf{x}$ is classified as a guidewire segment if $P(\mathbf{x}) > 0.5$, or as the background otherwise. Also to detect line segments at different orientations, images are rotated at 30 discretized orientations for detection. Figure 2.(b) shows an example of line segments detected in one frame.

2.2 Global and local rigid tracking

In the hierarchical guidewire tracking, the rigid tracking aims at searching the rigid motion of a guidewire between two successive frames, using primitive guidewire features, i.e., the detected line segments as described in Section 2.1. In guidewire tracking, we use the segments on a guidewire at the previous frame as the template, denoted as T. The line segments detected at the current frame are used as the observed primitive features, denoted as I. Given the template T and

the observation I, the rigid tracking is to find the best matching between T and I under a rigid motion model. The rigid tracking is further formalized as the maximization of a matching score, which is defined as E_m in Eqn. (2):

$$E_m(\overrightarrow{u}) = \sum_i \sum_j P(I(j)) exp\{-\frac{|T(i;\overrightarrow{u}) - I(j)|^2}{2\sigma^2}\}. \quad (2)$$

In Eqn. (2), the template and observation are represented as their spatial position, and $\overrightarrow{u}$ is the parameter of a rigid transformation. $T(i;\overrightarrow{u})$ denotes the i-th segment of the template under the rigid transformation $\overrightarrow{u}$, and $I(j)$ denotes the j-th segment of the current observation. $P(I(j))$ is the probabilistic output from the PBT based guidewire segment detector, indicating the confidence of the j-th segment. The Euclidean distance $|T(i;\overrightarrow{u}) - I(j)|$ is used to measure the distance between a template and guidewire primitive features under the rigid motion parameter $\overrightarrow{u}$, and σ is the kernel bandwidth. By varying the kernel bandwidth σ, the matching score can be computed at different resolutions. The rigid tracking is therefore to find the best rigid transformation $\overrightarrow{t}$ that maximize the matching score E_m, i.e., $\overrightarrow{t} = \arg\min_{\overrightarrow{u}} E_m(\overrightarrow{u})$.

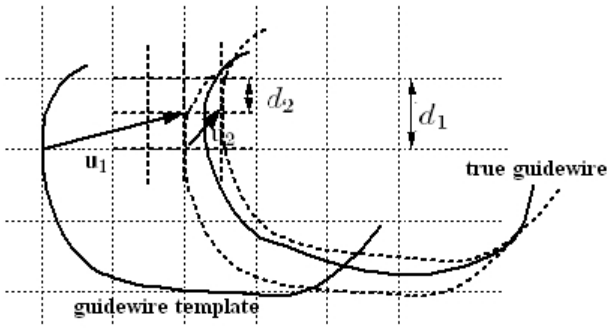

Figure 3. Multi-resolution rigid tracking with variable kernel bandwidths. The rigid tracking started from a template, and ends at position close to the true guidewire, up to an error caused by deformable motions. The dotted curves represent intermediate tracking results

Computation of the matching score in Eqn. (2) can be costly, when there are many detected segments in an image. For computational efficiency, we assume that a rigid motion is mainly caused by the translation, and the energy minimization of Eqn. (2) can be efficiently implemented by using variable kernel bandwidths in the maximization of Eqn. (2). As illustrated in Fig. 3, the rigid tracking is performed at multiple resolutions, with decreased search intervals $\{d_1 > d_2 > ... > d_T\}$ at an image grid. During the multi-resolution tracking, the corresponding bandwidth in Eqn. (2) varies accordingly, denoted as σ_i. At lower resolutions, we use larger kernel bandwidths to avoid missing tracking caused by larger sampling intervals; and at higher resolutions, we use smaller kernel bandwidths to obtain finer tracking results. In our method, we set $\sigma_i = d_i, i = 1, ..., T$, to adapt the multi-resolution tracking.

Moreover, the rigid tracking is performed at both global and local scales. At the global scale, the whole guidewire is tracked, while at the local scale, a whole guidewire is divided into several local segments for rigid tracking. The rigid tracking at the global and local scales both follows the same formalization as Eqn. (2). By the two-stage tracking, a guidewire is roughly tracked at the current frame. An example of global and local rigid tracking is shown in Figure 2.(c).

2.3 Non-rigid tracking

Starting from the guidewire aligned by the rigid tracking, the non-rigid tracking further refines the guidewire shape to recover the non-rigid motions of a guidewire. In the non-rigid tracking, we also want to maximize a matching score between a guidewire template and the observed guidewire primitive features. However, different from the rigid tracking, the non-rigid tracking tries to recover non-rigid motion parameters. Since this method does not assume any 3D projection information and priors of the guidewire shape, the guidewire shape and motion at a 2D plane is very flexible. To prevent the possible over-deformation of a guidewire, the matching score in the non-rigid tracking is a combination of a matching

score between a template and current guidewire features, and smoothness constraints that are imposed on the guidewire shape. Therefore, the matching score $E(\overrightarrow{u})$ of a non-rigid motion parameter $\overrightarrow{u}$ is defined in Eqn. (3):

$$\begin{aligned} E() &= E_m(\overrightarrow{u}) + E_s(\overrightarrow{u}) \\ &= \sum_i \sum_j exp\{-\frac{|T(i;\overrightarrow{u}) - I(j)|^2}{2\sigma^2}\} + \alpha \int |\frac{d\Gamma(\overrightarrow{u})}{ds}|^2 ds + \beta \int |\frac{d^2\Gamma(\overrightarrow{u})}{ds^2}|^2 ds. \end{aligned} \quad (3)$$

In Eqn. (3), $E_m(\overrightarrow{u})$ is a matching score, which is defined in the same way as in the rigid tracking. The only difference is that the transformation $\overrightarrow{u}$ in Eqn. (3) is non-rigid and can be very flexible. $E_s(\overrightarrow{u})$ is a smoothness constraint term. It consists of two parts from the first-order and second-order derivatives of the guidewire curve under the non-rigid deformation $\overrightarrow{u}$. α and β are coefficients to balance the energy terms of matching error and of smoothness constraints.

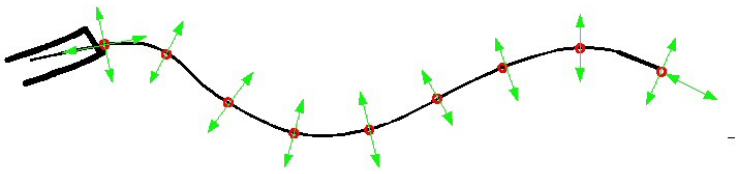

Figure 4. Non-rigid guidewire tracking. The control points (the red dots) on a guidewire spline deform along normal directions, and the two guidewire ends deform along both the normal and tangent directions

To find the non-rigid guidewire motion $\overrightarrow{u}$, the non-rigid tracking method takes the scheme that is similar to the Snakes algorithm.[2] Due to the flexibility of guidewire motion, the search space of the non-rigid motion parameter $\overrightarrow{u}$ is high dimensional. To reduce the dimensionality of the searching space, we deform control points on the guidewire body along normal directions, and the end of guidewire along both the tangent and normal directions, as illustrated in Fig. 4. But still, to exhaustively explore such a deformation space is formidable considering computational complexity. For example, if there are 20 control points, and each control point has 10 deformation candidates, the searching space contains 10^{20} candidates. Instead of parallelly searching or sampling the search space, our method searches guidewire deformation sequentially. At each step, only one control point deforms to achieve a maximum matching score. The sequential deformation will iterate until the maximum number of iterations is reached or it converges. The same as rigid tracking, the multi-resolution searching strategy is applied during the non-rigid tracking. The sequential searching strategy in most cases leads to an optimal solution, because the rigid tracking has roughly aligned the guidewire near the true shape. After the non-rigid tracking, a guidewire is finely tracked from the previous frame to the current frame. An example of final tracking result can be seen in Figure 2. (c).

3. QUANTITATIVE PERFORMANCE EVALUATION

3.1 Data and evaluation protocol

The tracking algorithm is evaluated on a set of fluoroscopic sequences. There are totally 47 sequences in the test set. The frame size of each sequence is 512*512 or 600*600, with the pixel size between 0.184 mm and 0.278 mm. Those sequences have various length, ranging from 5 to 150 frames per sequence. There are totally more than 1000 frames in the test set. Those testing sequences cover a variety of interventional conditions, including low image contrast, thin guidewire, and contrast injection. For illustration, some exemplar frames in the test set are displayed in Figure 5.

To establish a ground truth for evaluation, we manually annotate the whole body of guidewire in those sequences. An annotated guidewire starts from a guiding catheter tip, and ends at a guidewire tip. Also for the purpose of evaluating tracking performance, the annotation at the first frame of each sequence is used for initializing guidewire tracking. After the first frame, guidewire is continuously tracked through sequences. In clinical applications where an automated processing is desirable, the guidewire can be detected at the first frame automatically or interactively using the guidewire detection methods in our previous work.[6,11]

To comprehensively and quantitatively evaluate the performance of guidewire tracking, we define a set of metrics, including **guidewire body tracking precision**, **tip tracking precision** and **missing tracking rate**. Their definitions and meanings are explained as follows.

1. The **guidewire body tracking precision** is defined as the averaged shortest distance from points on the tracked guidewire to the annotated guidewire. Such a precision describes how close the tracked guidewire is to the ground truth. Under some cases, there could be visible guidewire inside the guiding catheter, although such guidewire is excluded from our annotation. This part of error has been excluded in the evaluation of guidewire body tracking precision.

2. The **missing tracking rate** is used to describe the percentage of actual guidewire that have not been identified during tracking. It is defined as follows. A miss-tracking point on an annotated guidewire is the point whose shortest distance to the tracked guidewire is greater than a pre-set threshold (3 pixel, i.e. 0.55mm, is set in this evaluation.) The missing rate is then the percentage of miss-tracked points on the annotated guidewire.

3. The **tip tracking precision** is defined as the distance between a tracked guidewire tip and it corresponding annotated tip. Since the pose of the guidewire tip is important in image guided interventions, its tracking accuracy is evaluated.

3.2 Evaluation Results

Figure 5 shows tracking results in some fluoroscopic sequences. It demonstrates that our method can successfully track the guidewires, even for those sequences with low visibility (Figure 5. (a) and (b)), background distraction (Figure 5. (c)), and contrast injection (Figure 5.(d)). For quantitative evaluations, three types of metrics, as defined in Section 3.1, are computed on the test set. We calculate the mean, median, and standard deviations of the three metrics over all the frames in the 47 sequences. The quantitative results are summarized in Table 1.

Table 1. Quantitative evaluation of guidewire (GW) tracking

Evaluation metrics	median	mean	std
GW Body Tracking Prec. (in pixels)	0.966	1.788	4.015
GW Body Tracking Prec. (in mm)	0.195	0.369	0.993
GW Missing Tracking Rate	9.25%	11.7%	14.07%
GW Tip Tracking Prec. (in pixels)	3.792	9.060	15.427
GW Tip Tracking Prec. (in mm)	0.728	1.946	3.807

As shown in Table 1, the mean of the guidewire body tracking precision is around 1.8 pixels, i.e., less than 0.4mm. Being robust to some difficult cases, the median of the guidewire body tracking precision is even less than 0.18mm. This demonstrates that our tracking method provides accurate results, and can greatly help cardiac interventions. The mean of the missing tracking rate is about 11.7%, which means the most parts of guidewires have been successfully tracked. The tracking at guidewire tips is more difficult than the body tracking, because there is more background noise around guidewire tips. The median of the guidewire tip tracking precision is 3.8 pixels, i.e., less than 0.8mm. This method runs at less than 1 second for one frame at a Core 2 Duo 2.0GHz computer. With further optimization of implementation, the method can achieve a near real-time speed for interventional applications.

4. CONCLUSION

This paper presents a hierarchical framework of guidewire tracking in fluoroscopy for image guided interventions. Our method has applied learning based method to detect guidewire segments, and hierarchically track guidewire motion from coarse to fine, and from rigid to non-rigid. The method has been validated on a test set containing real interventional sequences, and evaluations demonstrate that this method provides robust and accurate tracking results. Our future work will be applying the guidewire tracking to various clinical applications, e.g., breathing motion compensation.

REFERENCES

[1] Yilmaz, A., Javed, O., and Shah, M., "Object tracking: A survey," *ACM Comput. Surv.* **38**(4), 13 (2006).

[2] Kass, M., Witkin, A., and Terzopoulos, D., "Snakes: Active contour models," *International Journal of Computer Vision* **1**(4), 321–331 (1987).

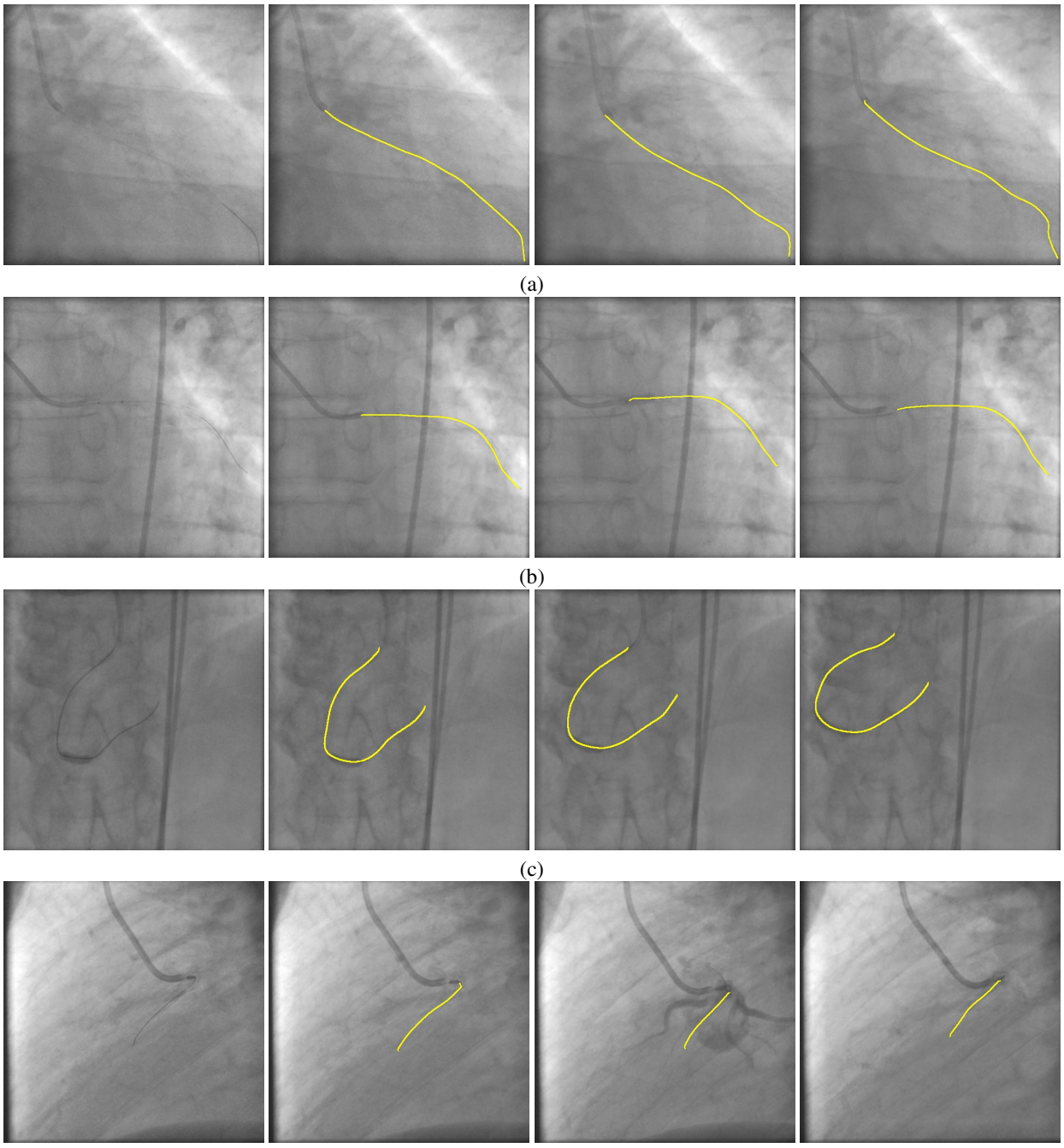

Figure 5. Some guidewire tracking results. In each graph, the left image is the first frame of a sequence, and right images show tracking results (yellow curves) at some frames. The figures are best viewed in color

[3] Shi, Y. and Karl, W. C., "Real-time tracking using level sets," in [*IEEE Computer Society Conference on Computer Vision and Pattern Recognition*], **2**, 34–41, IEEE Computer Society, Washington, DC, USA (2005).

[4] Palti-Wasserman, D., Brukstein, A. M., and Beyar, R., "Identifying and tracking a guide wire in the coronary arteriesduring angioplasty from x-ray images," *IEEE Trans. Biomedical Engineering* **44**(2), 152–164 (1997).

[5] Baert, S. A. M., Viergever, M. A., and Niessen, W. J., "Guide wire tracking during endovascular interventions," *IEEE Trans. Med. Imaging* **22**(8), 965–972 (2003).
[6] Barbu, A., Athitsos, V., Georgescu, B., Boehm, S., Durlak, P., and Comaniciu, D., "Hierarchical learning of curves application to guidewire localization in fluoroscopy," in [*CVPR*], (2007).
[7] Tu, Z., "Probabilistic boosting-tree: Learning discriminative models for classification, recognition, and clustering," in [*ICCV*], 1589–1596 (2005).
[8] Freund, Y. and Schapire, R. E., "A decision-theoretic generalization of on-line learning and an application to boosting," in [*European Conference on Computational Learning Theory*], 23–37 (1995).
[9] Viola, P. and Jones, M., "Robust real-time object detection," *Interntional Workshop on Statistical and Computational Theories of Vision* **57**(2), 137–154 (2004).
[10] Friedman, J., Hastie, T., and Tibshirani, R., "Additive logistic regression: a statistical view of boosting," *The Annals of Statistics* **28**(2), 337–374 (2000).
[11] Mazouer, P., Chen, T., Zhu, Y., Wang, P., Durlak, P., Thiran, J.-P., and Comaniciu, D., "User-constrained guidewire localization in fluoroscopy," in [*Medical Imaging: Image Processing*], *Proc. SPIE* (2009).